Inorg. Chem. **2002**, *41*, 4025–4028

Metalla-Supramolecular Rectangles as Electron Reservoirs for Multielectron Reduction and Oxidation

Wolfgang Kaim,*,† Brigitte Schwederski,† Akbey Dogan,† Jan Fiedler,‡ Christopher J. Kuehl,*,§ and Peter J. Stang*,§

Institut für Anorganische Chemie, Universität Stuttgart, Pfaffenwaldring 55, D-70550 Stuttgart, Germany, J. Heyrovsky Institute of Physical Chemistry, Academy of Sciences of the Czech Republic, Dolejškova 3, CZ-18223 Prague, Czech Republic, and Department of Chemistry, University of Utah, Salt Lake City, Utah 84112-0850

Received February 12, 2002

The electron-transfer capacity of molecular rectangle ions $[Pt^{II}_4(PEt_3)_8(\mu\text{-anth}^{2-})_2(\mu\text{-L})_2]^{4+}$ with anth = anthracene-1,8-diyl and L = 4,4′-bipyridine (bp) or 1,2-bis(4-pyridyl)ethene (bpe) was investigated in acetonitrile and dichloromethane using cyclic voltammetry, EPR, and UV–vis–near-IR spectroelectrochemistry. The compounds can be reversibly reduced, first in a two-electron process and then via two closely separated one-electron steps. Oxidation was also possible at rather low potentials in a reversible two-electron step, followed by an electrochemically irreversible process. The spectroscopic results indicate reduction at the neutral acceptor ligands L and oxidation at the formally dianionic anthracene "clips". In contrast, the prototypical molecular square $\{[Pt(triphos)(\mu\text{-bp})]_4\}^{8+}$ undergoes only irreversible reduction.

Introduction

Molecular squares and rectangles with metal corners and unsaturated ligand sides have become a representative class of "supramolecular" species.[1] In addition to the remarkable self-assembly formation reactions and the unusual structures, these systems have attracted attention due to their potential for the molecular recognition of substrates,[2] for interaction with light (antenna function),[3] and for intramolecular magnetic exchange coupling.[4] However, there have not been many studies of the electron-transfer behavior of molecular squares or rectangles;[1,3] a recent investigation of the neutral tetrarhenium(I) rectangle $[Re_4(CO)_{12}(\mu\text{-bp})_2(\mu\text{-bpym})_2]$ (bp = 4,4′-bipyridine and bpym = 2,2′-bipyrimidine) has revealed the stepwise and site-specific uptake of eight electrons by the bridging ligands in this supramolecule.[5]

Using two recently reported[6] molecular rectangle ions $[Pt^{II}_4(PEt_3)_8(\mu\text{-anth}^{2-})_2(\mu\text{-L})_2]^{4+}$ (as hexafluorophosphate salts) with four platinum(II) corners, two facing acceptor sides L (L = bp (**1**) or L = bpe (**2**)), and two anthracene-1,8-diyl

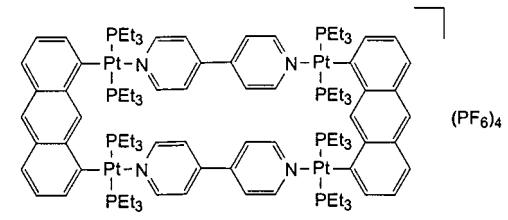

1

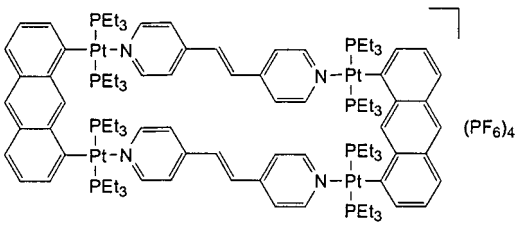

2

side "clips", we can now report that these supramolecular entities can also undergo site-specific oxidation in addition

* Authors to whom correspondence should be addressed. E-mail: kaim@iac.uni-stuttgart.de (W.K.).
† Universität Stuttgart.
‡ Academy of Sciences of the Czech Republic.
§ University of Utah.

(1) (a) Stang, P. J.; Olenyuk, B. *Acc. Chem. Res.* **1997**, *30*, 502. (b) Leininger, S.; Olenyuk, B.; Stang, P. J. *Chem. Rev.* **2000**, *100*, 853.
(2) (a) Whiteford, J. A.; Lu, C. V.; Stang, P. J. *J. Am. Chem. Soc.* **1997**, *119*, 2524. (b) Whiteford, J. A.; Stang, P. J.; Huang, S. D. *Inorg. Chem.* **1998**, *37*, 5595. (c) Beer, P. D.; Gale, P. A. *Angew. Chem.* **2001**, *115*, 503; *Angew. Chem., Int. Ed.* **2001**, *40*, 486. (d) Johnson, D. W.; Raymond, K. N. *Supramol. Chem.* **2001**, *13*, 639.
(3) (a) Slone, R. V.; Benkstein, K. D.; Bélanger, S.; Hupp, J. T.; Guzei, I. A.; Rheingold, A. L. *Coord. Chem. Rev.* **1998**, *171*, 221. (b) Sun, S.-S.; Lees, A. J. *Inorg. Chem.* **1999**, *38*, 4181.
(4) Campo-Fernandez, C. S.; Clérac, R.; Dunbar, K. R. *Angew. Chem.* **1999**, *111*, 3685; *Angew. Chem., Int. Ed.* **1999**, *38*, 3477.

10.1021/ic020122n CCC: $22.00
Published on Web 07/02/2002

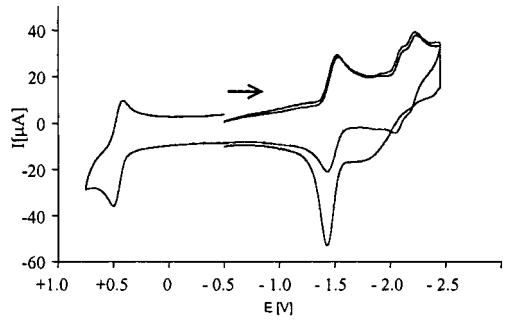

Figure 1. Cyclic voltammograms of compound **1** in CH_3CN/0.1 M Bu_4NPF_6 at a scan rate of 200 mV/s. Electrode adsorption of the four-electron-reduced species is evident from the increase of the return peak at −1.4 V after a delay time of 5 s at −2.4 V.

to multiple reduction. Spectroelectrochemical techniques involving an optically transparent thin-layer electrode (OTTLE) cell as well as EPR spectroscopy of the paramagnetic intemediates served to establish the location of individual electron-transfer processes.

We also report results from studies of the prototypical, structurally well characterized molecular square $\{[Pt(triphos)(\mu\text{-bp})]_4\}^{8+}$ (**3**),[7] which helped to start the research field.[1]

Experimental Section

Complexes. The tetraplatinum(II) complexes **1**,[6] **2**,[6] and **3**[7] have been described.

Instrumentation. EPR spectra were recorded in the X band on a Bruker System ESP 300 equipped with a Bruker ER035M gauss meter and a HP 5350B microwave counter. UV−vis−near-IR absorption spectra were recorded on a Bruins Instruments Omega 10 spectrophotometer. Cyclic voltammetry was carried out at a 200 mV/s scan rate in CH_3CN/0.1 M Bu_4NPF_6 using a three-electrode configuration (glassy-carbon working electrode, Pt counter electrode, Ag/AgCl reference) and a PAR 273 potentiostat and function generator. The ferrocene/ferrocenium couple served as internal reference. Coulometry was performed by employing a mercury-pool working electrode in an electrolytic vessel with the platinum counter electrode in a compartment separated by sintered glass and an Ag/AgCl reference. Spectroelectrochemical measurements were performed in CH_3CN/0.1 M Bu_4NPF_6 using an optically transparent thin-layer electrode (OTTLE) cell[8] for UV−vis spectra and in CH_2Cl_2/0.1 M Bu_4NPF_6 using a two-electrode capillary for EPR studies.[9]

Results and Discussion

The compounds **1** and **2** were subjected to cyclic voltammetry in acetonitrile/0.1 M Bu_4NPF_6 at scan rates ranging from 0.05 to 50 V/s. The representative cyclic voltammogram of **1** (Figure 1) exhibits three sets of reversible two-electron waves (one oxidation and two reduction waves), of which the one at the most negative potential shows a clear splitting, here by about 120 mV, into two one-electron processes. Two-electron consumption was verified by controlled-potential coulometry at the first reduction wave. Similar behavior was observed for **2** and for rectangular $[Re_4(CO)_{12}(\mu\text{-bp})_2(\mu\text{-bpym})_2]$ in DMF.[5]

Table 1. Electrochemical[a] and Spectroscopic[b,c] Properties of Complex Ions $[Pt_4(PEt_3)_8(\mu\text{-anth})_2(\mu\text{-L})_2]^{n+}$

	L = bp	L = bpe
	Reduction	
$E(4+/2+)$	−1.44 (69)	−1.36 (67)
$E(2+/+)$	−2.05 (66)	−1.62 (62)
$E(+/0)$	−2.17[d]	−1.67[d]
$\lambda_{max}/\epsilon(4+)$	409/5200, 388/5500, 370/4800, 267/5400	410/4800, 388/5000, 370/4000, 320/18 000, 269/54 000
$\lambda_{max}/\epsilon(2+)$	849/1000, 755/1400, 631/9000, 581/11 000, 548 sh, 416 sh, 403/27 000, 265/43 500	784/13 000, 702/13 200, 601/8500, 508/44 500, 490 sh, 267/39 500
$g_{iso}(2+)$	2.0043[e]	2.0032[f]
$g_1(2+)$	2.042	2.037
$g_2(2+)$	2.004[g]	2.004[h]
$g_3(2+)$	1.952	1.959
	Oxidation	
$E(4+/6+)$	0.49	0.55
$E_{p,a}(6+)$	1.17	1.28
	L = bp	L = bpe
$\lambda_{max}/\epsilon(6+)$	1046/6000, 923/2500, 663/1600, 602/2200, 560 sh, 413/3300, 322/18 400, 265/36 000	1048/6000, 924/2500, 662/1700, 602/2200, 560 sh, 413/3100, 324/33 000, 265/22 000
g_{iso}[i]	2.018	2.019
ΔH_{pp}[j]	2.1	0.7

[a] From cyclic voltammetry in CH_3CN/0.1 M Bu_4NPF_6 at a scan rate of 200 mV/s; potentials in V vs $[Fe(C_5H_5)_2]^{+/0}$ and peak potential differences in mV (in parentheses). [b] From spectroelectrochemistry in 0.1 M Bu_4NPF_6 solutions of CH_3CN (UV−vis−near-IR absorption spectra) and CH_2Cl_2 (EPR spectra). **g** tensor components were measured in frozen solution at 110 K. [c] Wavelengths λ_{max} in nm and molar extinction coefficients ϵ in M^{-1} cm^{-1}. [d] Electrode adsorption. [e] Partially resolved spectrum with smallest detectable coupling at about 0.1 mT. [f] Partially resolved spectrum with smallest detectable coupling at about 0.2 mT. [g] $a_2(^{195}\text{Pt}) \approx 5.0$ mT. [h] $a_2(^{195}\text{Pt}) \approx 4.5$ mT. [i] Unresolved signal at 298 and 110 K. [j] Peak-to-peak line width of room-temperature spectrum in mT.

After acceptance of four electrons the then neutral species $[Pt_4(PEt_3)_8(\mu\text{-anth})_2(\mu\text{-L})_2]$ shows slow adsorption at the cathode (onset of electrocrystallization), as is evident from the typical cyclic voltammetric desorption response after a time delay (Figure 1).

After the first reversible two-electron oxidation wave a second oxidation feature is observed for both **1** and **2** ions at high potentials; however, this process is electrochemically irreversible. The redox potential data are summarized in Table 1 and Scheme 1.

Despite its high positive charge of 8+, the compound **3** is reduced only irreversibly at $E_{p,c} = -1.43$ V, a value essentially identical with $E_{1/2}$(red) for **1**. Obviously, the anionic anthracene clips provide the chemical stability necessary for multiple reversible redox processes. Their absence (in **3**) or their deactivation through four-electron oxidation of **1** or **2** results in irreversible electron transfer.

The electrode potentials alone do not unambiguously reveal the sites of the individual electron-transfer processes, although previous experience[5,11] suggests reversible reduction of bridging 4,4′-bipyridine and facile oxidation of dianionic

(5) Hartmann, H.; Berger, S.; Winter, R.; Fiedler, J.; Kaim, W. *Inorg. Chem.* **2000**, *39*, 4977.
(6) Kuehl, C. J.; Huang, S. D.; Stang, P. J. *J. Am. Chem. Soc*. **2001**, *123*, 9634.
(7) Stang, P. J.; Cao, D. H. *J. Am. Chem. Soc.* **1994**, *116*, 4981.
(8) Krejcik, M.; Danek, M.; Hartl, F. *J. Electroanal. Chem. Interfacial Electrochem.* **1991**, *317*, 179.
(9) Kaim, W.; Ernst, S.; Kasack, V. *J. Am. Chem. Soc.* **1990**, *112*, 173.
(10) Vlcek, A. A., *Coord. Chem. Rev.* **1982**, *43*, 39.

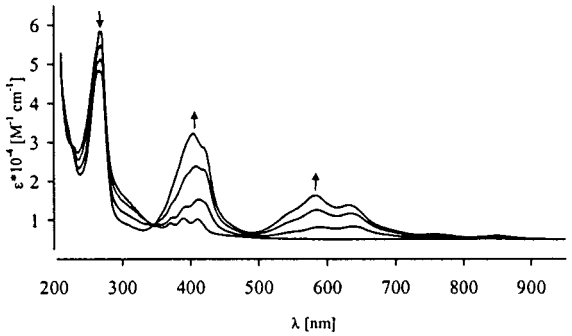

Figure 2. Spectral change during the reduction of **1** in CH_3CN/0.1 M Bu_4NPF_6: $[Pt_4(PEt_3)_8(\mu\text{-anth})_2(\mu\text{-bp})_2]^{4+\rightarrow 2+}$.

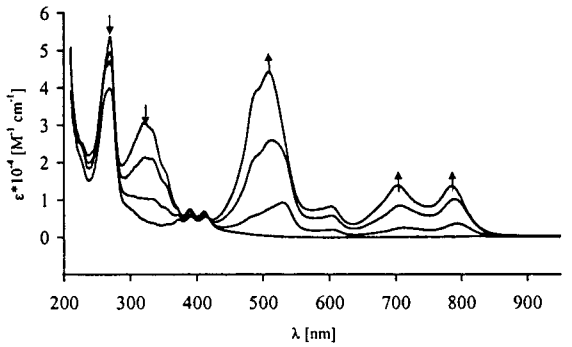

Figure 3. Spectral change during the reduction of **2** in CH_3CN/0.1 M Bu_4NPF_6: $[Pt_4(PEt_3)_8(\mu\text{-anth})_2(\mu\text{-bpe})_2]^{4+\rightarrow 2+}$.

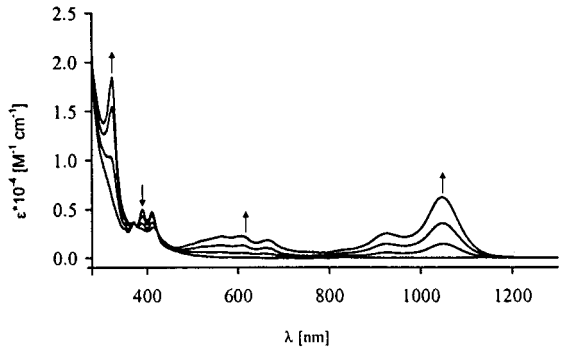

Figure 4. Spectral change during the oxidation of **1** in CH_3CN/0.1 M Bu_4NPF_6: $[Pt_4(PEt_3)_8(\mu\text{-anth})_2(\mu\text{-bp})_2]^{4+\rightarrow 6+}$.

anthracene-based ligands. This behavior would indicate spatially simultaneous electron-transfer proceses at corresponding equivalent sides of the molecular rectangles **1** and **2** (see Scheme 1). The two-electron character of the first oxidation or reduction and the observed (Table 1) separation close to 60 mV of corresponding peaks implies negligible interaction[12] across the molecular rectangles, a result which is confirmed by spectroelectrochemistry and EPR. The splitting of the second two-electron reduction wave (Figure 1) is probably enhanced by the increased negative charge on the ligands[10] (Coulombic repulsion) and by the closer proximity of the bp or bpe sides in the rectangles (clip effect). We do not think that the splitting is due to an ECE mechanism (inserted chemical processes), since varying the cyclic voltammetry scan rates did not reveal any significant change of the ratio of peak heights.

We therefore used OTTLE spectroelectrochemistry[8] in the UV−vis−near-IR region because the $bp^{\bullet-}$ chromophore[13,14a] has a distinct band structure in the visible region with wavelengths at about 600 nm, familiar from the "methyl viologen" coloring. The $bpe^{\bullet-}$ ion has absorptions at slightly higher wavelengths (lower energies).[14b] The larger anthracene π radical chromophore should exhibit absorptions at still higher wavelengths in the near-infrared region.[14c]

Figures 2 and 3 illustrate the UV−vis−near-IR spectroelectrochemical responses of **1** and **2** on two-electron reduction; Figure 4 shows the effect of the two-electron oxidation of **1**. The relevant data are listed in Table 1.

For **1** the first two-electron reduction process causes the emergence of a vibrationally structured band system around 600 nm and another intense band at 403 nm. The latter overlaps with the typically structured anthracene $\pi\rightarrow\pi^*$ bands around 390 nm. This pattern is very similar to that of $bp^{\bullet-}$ in MTHF (λ_{max} = 585 and 385 nm).[13,14a] Further stepwise one-electron reduction causes these bands to diminish; the neutral product of the overall four-electron reduction could not be characterized due to the aforementioned electrode adsorption.

A similar behavior but with different (i.e. bathochromically shifted) absorption maxima at 784, 702, 601, and 508 nm was observed for **2** (Figure 3, Table 1), confirming L as the site for reduction: $bpe^{\bullet-}$ in MTHF has λ_{max} = 746, 675, 568, and 488 nm.[14b]

Two-electron oxidations of both **1** and **2** yield almost identical results (Table 1), supporting the invariant electron-rich anthracene-1,8-diyl dianion as the site of electron loss. The spectrum shows an intense long-wavelength band at about 1050 nm and another band system at about 600 nm (Figure 4). Oxidation beyond the electrochemically irreversible second wave produced a new band around 690 nm; however, the spectrum of the first intermediate (Figure 4) is retained on rereduction to 80%, suggesting a chemically largely reversible reaction following the second oxidation.

In situ EPR spectroscopy of the two-electron intermediates of the reduction and oxidation gave normal spectra (Figure 5, Table 1), indicating little spin−spin interaction across the rectangular structures. Accordingly, half-field signals from triplet states could not be detected in frozen solutions at 110 K.

Reduction of **1** yields a partially resolved EPR spectrum at room temperature (Figure 5) with an isotropic g factor of 2.0046: i.e., close to g = 2.0030 for the free $bp^{\bullet-}$ ligand and not very different from values of corresponding dinuclear complexes.[11] The hyperfine structure could not be completely analyzed due to insufficient resolution and a high theoretical number of lines if coupling from ^1H ($I = {}^1/_2$, 2 × 4H), ^{14}N

(11) (a) Kaim, W. *J. Organomet. Chem.* **1983**, *241*, 157. (b) Kaim, W. *Inorg. Chim. Acta* **1981**, *53*, L151. (c) Kaim, W. *Chem. Ber.* **1982**, *115*, 910. (d) Bruns, W.; Kaim, W.; Waldhör, E.; Krejcik, M. *Inorg. Chem.* **1995**, *34*, 663.
(12) (a) Flanagan, J. B.; Margel, S.; Bard, A. J.; Anson, F. C. *J. Am. Chem. Soc.* **1978**, *100*, 4248. (b) Ammar, F.; Saveant, J. M. *J. Electroanal. Chem. Interfacial Electrochem.* **1973**, *47*, 2155.
(13) (a) Hünig, S.; Berneth, H. *Top. Curr. Chem.* **1980**, *92*, 1. (b) Summers, L. A. *The Bipyridinium Herbicides*; Academic Press: New York, 1980.
(14) (a) Shida, T. *Electronic Absorption Spectra of Radical Ions*; Elsevier: Amsterdam, 1988; p 198. (b) *Ibid*., p 202. (c) *Ibid*., p 69.

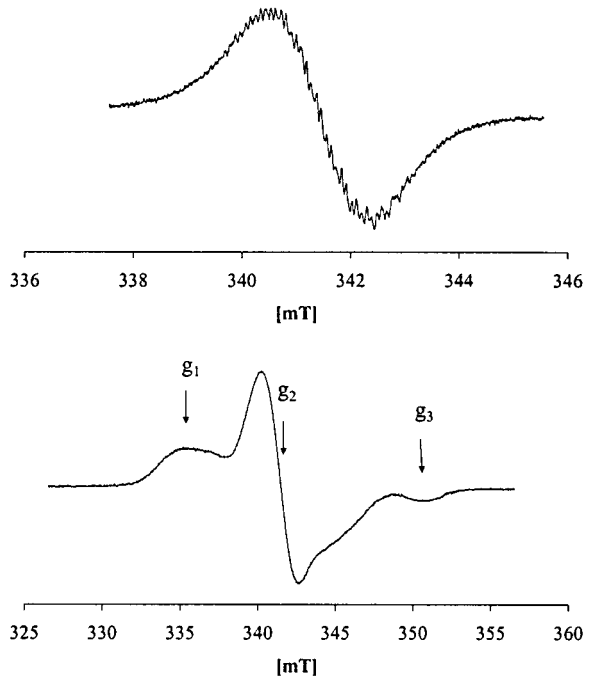

Figure 5. EPR spectra of electrogenerated $[Pt_4(PEt_3)_8(\mu\text{-anth})_2(\mu\text{-bp})_2]^{2+}$ in CH_2Cl_2/0.1 M Bu_4NPF_6 at 298 K (top) and 110 K (bottom; shoulders of g_2 due to ^{195}Pt coupling).

($I = 1$, 2 N), ^{31}P ($I = {}^1/_2$, 4 P), and ^{195}Pt nuclei (34% natural abundance, $I = {}^1/_2$, 2 Pt) is to be considered. The smallest coupling constant is ca. 0.1 mT, in agreement with typical values for $a(H^{2,6})$ in the compounds $(bp^{\bullet-})(ML_n)_2$.[11] In the glassy frozen state, the two-electron-reduced form of **1** shows g components at $g_1 = 2.0414$, $g_2 = 2.0040$, and $g_3 = 1.9515$, a rhombic g anisotropy which has been similarly observed for other platinum(II) complexes bridged by anion radical ligands.[15] A metal isotope coupling $a_2(^{195}Pt)$ of about 4−5 mT is detected, which is a magnitude typical for such hyperfine values in anion radical complexes of Pt^{II}.[15]

Comparable EPR effects were observed in the reduction of **2** as quantified in Table 1; the smallest observable coupling constant of about 0.2 mT has similarly been observed for $bpe^{\bullet-}$ and some of its dinuclear complexes.[11c]

Oxidation of both **1** and **2** yields unresolved EPR spectra in solution and in the glassy frozen state. The isotropic g values of about 2.019 indicate higher participation of the platinum(II) heavy-metal centers with their large spin−orbit coupling constant[16] at the singly occupied MO; however, no g anisotropy could detected in the glassy frozen state at X-band frequency. Apparently, the stronger covalency of the Pt−C bonds from the metal to the anionic carbon radical ligand causes an increase of g_{iso} but a decrease of the metal hyperfine coupling.[17]

On the basis of the combined spectroelectrochemical and EPR information we can suggest Scheme 1 for the sequence of site-specific electron transfer to the molecular rectangles **1** and **2**.

Scheme 1

$$\uparrow \quad -2\,e^- \text{ (irr., } E_{pa} = 1.17 \text{ V(bp) or } 1.28 \text{ V (bpe))}$$

$$[Pt^{II}{}_4(PEt_3)_8(\mu\text{-anth}^{\bullet-})_2(\mu\text{-L})_2]^{6+}$$

$$+2\,e^- \downarrow\uparrow \quad -2\,e^- \quad E(4+/6+) = 0.49 \text{ V (bp) or } 0.55 \text{ V (bpe)}$$

$$[Pt^{II}{}_4(PEt_3)_8(\mu\text{-anth}^{2-})_2(\mu\text{-L})_2]^{4+}$$

$$+2\,e^- \downarrow\uparrow \quad -2\,e^- \quad E(4+/2+) = -1.44 \text{ V (bp) or } -1.36 \text{ V (bpe)}$$

$$[Pt^{II}{}_4(PEt_3)_8(\mu\text{-anth}^{2-})_2(\mu\text{-L}^{\bullet-})_2]^{2+}$$

$$+e^- \quad \downarrow\uparrow \quad -e^- \quad E(2+/+) = -2.05 \text{ V (bp) or } -1.62 \text{ V (bpe)}$$

$$[Pt^{II}{}_4(PEt_3)_8(\mu\text{-anth}^{2-})_2(\mu\text{-L}^{\bullet-})(\mu\text{-L}^{2-})]^{+}$$

$$+e^- \quad \downarrow\uparrow \quad -e^- \quad E(+/0) = -2.17 \text{ V (bp) or } -1.67 \text{ V (bpe)}$$

$$[Pt^{II}{}_4(PEt_3)_8(\mu\text{-anth}^{2-})_2(\mu\text{-L}^{2-})_2]^{o}$$

While all evidence points to negligible interaction between the pairwise formed radical ligands in the primary two-electron-reduced or -oxidized species, the capacity of these supramolecules to accommodate several redox equivalents adds yet another function to their array of remarkable physical and chemical properties.

Acknowledgment. Financial support from the DFG and FCI (Germany) and from the NSF and NIH (USA) is gratefully acknowledged.

IC020122N

(15) (a) Klein, A.; Kaim, W.; Fiedler, J.; Zalis, S. *Inorg. Chim. Acta* **1997**, *264*, 269. (b) Klein, A.; Hasenzahl, S.; Kaim, W.; Fiedler, J. *Organometallics* **1998**, *17*, 3532.
(16) Weil, J. A.; Bolton, J. R.; Wertz, J. E. *Electron Paramagnetic Resonance*; Wiley: New York, 1994.
(17) For a related discussion see: Osborne, J. H.; Rheingold, A. L.; Trogler, W. C. *J. Am. Chem. Soc.* **1985**, *107*, 7945.